Open Access Full Text Article

ORIGINAL RESEARCH

Exploring the Relevance of Disulfidptosis to the Pathophysiology of Ulcerative Colitis by Bioinformatics Analysis

Zhe Xiong[1,2], Ying Fang[1,2], Shuangshuang Lu[1], Qiuyue Sun[1,3], Yuhui Sun[1,3], Pengcheng Yang[4,*], Jin Huang[1,*]

[1]Department of Gastroenterology, The Affiliated Changzhou No.2 People's Hospital of Nanjing Medical University, Changzhou, Jiangsu Province, People's Republic of China; [2]Graduate School of Dalian Medical University, Dalian, Liaoning Province, China; [3]Graduate School of Nanjing Medical University, Nanjing, Jiangsu Province, People's Republic of China; [4]Department of Gastroenterology, Hengshanqiao People's Hospital, Changzhou, Jiangsu Province, People's Republic of China

*These authors contributed equally to this work

Correspondence: Pengcheng Yang; Jin Huang, Email 496808936@qq.com; hj042153@hotmail.com

Background: Ulcerative colitis (UC) is a nonspecific inflammatory disease confined to the intestinal mucosa and submucosa, and its prevalence significantly increases each year. Disulfidptosis is a recently discovered new form of cell death that has been suggested to be involved in multiple diseases. The aim of this study was to explore the relevance of disulfidptosis in UC.

Methods: First, the UC datasets were downloaded from the Gene Expression Omnibus (GEO) database, and UC samples were typed based on upregulated disulfidptosis-related genes (DRGs). Then, weighted gene co-expression network analysis (WGCNA) was performed on the datasets and molecular subtypes of UC, respectively, to obtain candidate signature genes. After validation of the validation set and qRT-PCR, we constructed a nomogram model by signature genes to predict the risk of UC. Finally, single-cell sequencing analysis was used to study the heterogeneity of UC and to demonstrate the expression of DRGs and signature genes at the single-cell level.

Results: A total of 7 DRGs were significantly upregulated in the expression profiles of UC, and 180 UC samples were divided into two subtypes based on these DRGs. Five candidate signature genes were obtained by intersecting two key gene modules selected by WGCNA. After evaluation, four signature genes with diagnostic relevance (*COL4A1, PRRX1, NNMT,* and *PECAM1*) were eventually identified. The nomogram model showed excellent prediction ability. Finally, in the single-cell analysis, there were eight cell types (including B cells, T cells, monocyte, smooth muscle cells, epithelial cells, neutrophil, endothelial cells and NK cells) were identified. The signature genes were significantly expressed mainly in endothelial cells and smooth muscle cells.

Conclusion: In this study, subtypes related to disulfidptosis were identified, and single-cell analysis was performed to understand the pathogenesis of UC from a new perspective. Four signature genes were screened and a prediction model with high accuracy was established. This provides novel insights for early diagnosis and therapeutic targets in UC.

Keywords: ulcerative colitis, disulfidptosis, molecular clusters, WGCNA, nomogram

Introduction

Ulcerative colitis (UC) is a chronic idiopathic inflammatory disease involving the colorectal segment in which lesions are mainly confined to the colonic mucosa and submucosa in a continuous diffuse distribution.[1] Recently, the prevalence of UC has risen dramatically worldwide, greatly affecting the quality of life. Recurrent diarrhea, abdominal pain, fever, weight loss, and hematochezia are the main symptoms of UC.[2,3] In addition, the risk of colorectal cancer is significantly higher in some patients with UC who have recurring symptoms and a long course of disease.[4] Currently, the pathogenesis of UC is not fully understood but is primarily related to the environment, genetic susceptibility and intestinal microbial

2757

interactions leading to intestinal immune imbalance.[5,6] Therefore, we need to further shed light on the molecular mechanisms in UC to pave the way for the prevention, diagnosis, and treatment of UC.

Disulfidptosis is a newly defined cell death mechanism. In contrast to previous apoptosis, necroptosis, and ferroptosis, disulfidptosis is primarily associated with disulfide bonds in cells. The primary mechanism of disulfidptosis is that the supply of nicotinamide adenine dinucleotide phosphate (NADPH) is insufficient for the cell to reduce cystine to cysteine thereby causing disulfide stress, causing the collapse of abnormal disulfide bonds in the actin cytoskeleton, and eventually inducing cell death.[7] The study further demonstrated that the glucose transport (GLUT) inhibitor triggered disulfidptosis in cancer cells, which could effectively inhibit tumor growth without significant damage to normal tissues.[8] These studies suggested an important role for disulfidptosis in cancer. Similarly, the actin cytoskeleton is key pathological mechanisms in colitis. Therefore, we discuss here whether disulfidptosis also occurs in UC. Figure 1 demonstrates the pathway we constructed for disulfidptosis leading to the development of UC based on previously published literature.

In this article, we emphasized the significance of disulfidptosis in the pathogenesis of UC through bioinformatics analysis. First, we collected gene expression profiles in patients with UC and healthy patients via the Gene Expression Omnibus (GEO) database and divided 180 patients with UC into two clusters based on the expression level of 7 significantly upregulated disulfidptosis-related genes (DRGs). Subsequently, the key gene modules for disease and clusters were obtained by the weighted gene co-expression network analysis (WGCNA), and these two modules were overlapped to obtain candidate signature genes. A nomogram model was then constructed to predicts the risk of UC from validated signature genes. In addition, we attempted to investigate the correlation between signature genes and immune cells by ssGSEA (single sample gene set enrichment analysis). Finally, we examined the expression and distribution of DRGs and signature genes in single cells. Overall, our results are expected to further understand the biological mechanisms of disulfidptosis in UC and to provide personalized solutions for the management of UC.

Materials and Methods
Sources and Processing of Datasets

The UC datasets for this study were downloaded from the GEO public database (https://www.ncbi.nih.gov/geo/). In the database, patients with active UC were used as screening criteria to ensure the accuracy of the results of this study. In addition, datasets containing a high number of patients were merged and used as initial data. The GSE75214[9] dataset (UC, tissue type: intestinal mucosal from patients, N = 74; Controls, N = 22) was used for the GPL6244 platform. The GSE87473[10] dataset (UC, tissue type: intestinal mucosal from patients, N = 106; Controls, N = 21) was used for the
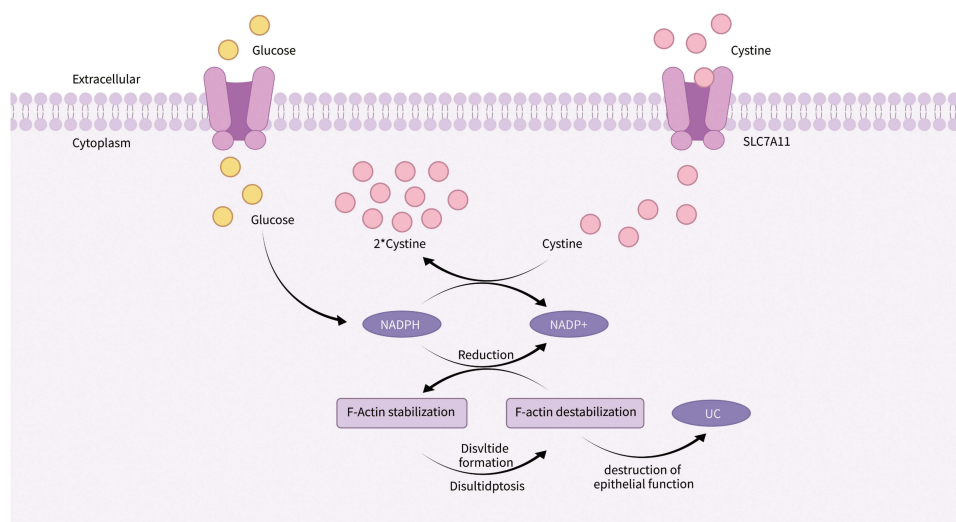

Figure 1 The increased NADP+/NADPH ratio in SLC7A11 highly expressed cells resulted in the inability of the cells to reduce cystine to cysteine, which in turn resulted in the contraction of the disulfide bonds of the actin cytoskeleton associated proteins, ultimately inducing disufidptosis. In addition, the collapse of the actin cytoskeleton led to the disruption of intestinal epithelial cells function, which in turn contributed to the development of ulcerative colitis.
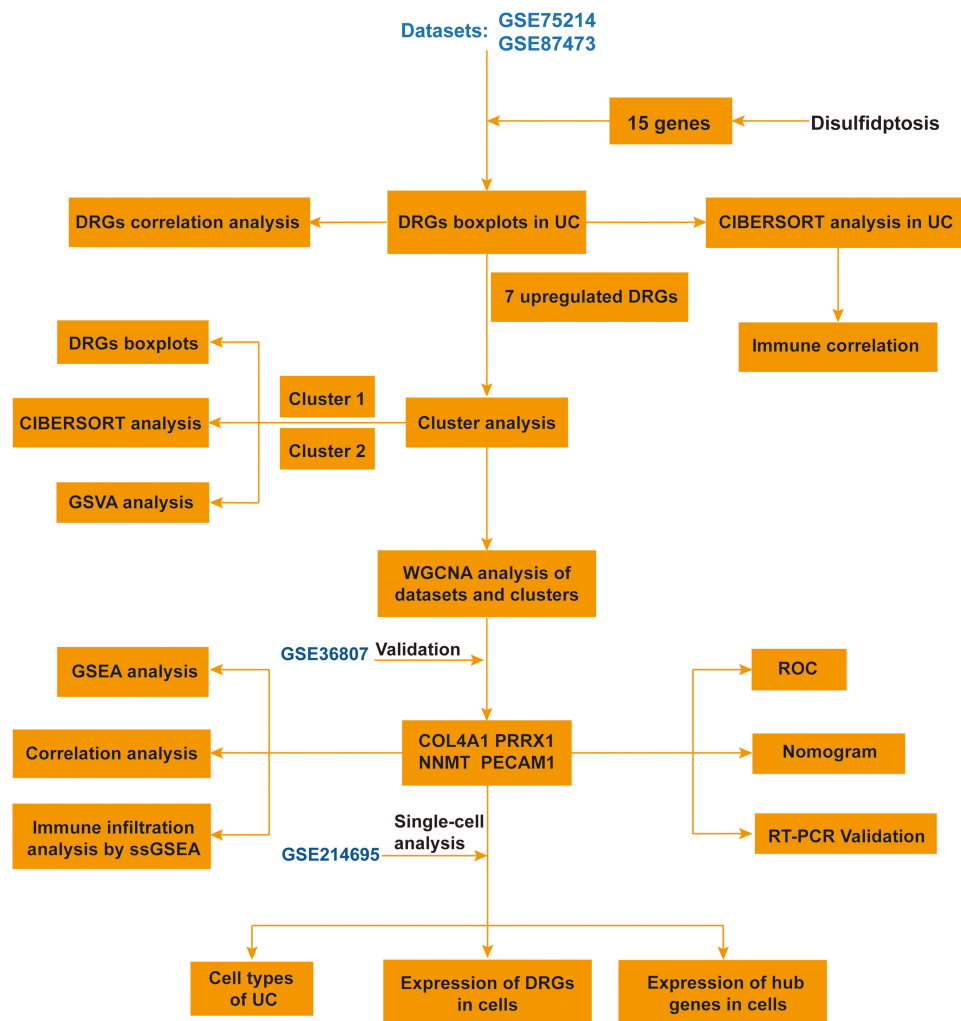
Figure 2 Flowchart of this study.

GPL13158 platform. The GSE36807[11] dataset (UC, tissue type: intestinal mucosal from patients, N = 21; Controls, N = 7) was used for the GPL570 platform. Figure 2 demonstrates the flowchart of this study. Subsequently, the GSE75214 and the GSE87473 datasets were merged and the batch effect in the gene expression profiles was eliminated by the comBat function of the "sva" R package. In a recent literature, the authors mentioned 15 genes that are overexpressed in cells undergoing disulfidptosis.[7] Table 1 shows the 15 DRGs and their functions. Boxplots were used to demonstrate the expression levels of all DRGs in UC and control samples.

Immune Cell Infiltration Analysis

Since immune imbalance is an essential element in the pathogenesis of UC, we further evaluated the abundance of different immune cell infiltration in UC and control groups using CIBERSORT immune cell infiltration analysis.[12] In order to explore the role of immune cells in disulfidptosis affecting UC, the correlation of the significantly expressed DRGs with immune cells was then investigated.

Identification and Exploration of Disulfidptosis-Related Subtypes in UC

Based on the significantly upregulated DRGs, we performed unsupervised hierarchical clustering analysis for 180 UC samples by the "ConsensuClusterPlus" R package,[13] and principal component analysis (PCA) using the "limma" and "ggplot2" R packages[14] to verify the clustering results. Next, significantly enriched molecular pathways were identified

Table 1 DRGs and the Functions of These Genes

Gene	Gene Function
FLNA	Cytoskeletal protein binding
FLNB	Repair vascular injuries
MYH9	Cell adhesion molecule
TLN1	Cytoskeletal protein binding
ACTB	Cytoskeletal protein binding
MYL6	Actin binding
MYH10	Actin binding
CAPZB	Actin binding
DSTN	Cytoskeletal protein binding
IQGAP1	Cell adhesion molecule
ACTN4	Actin binding
PDLIM1	Cytoskeletal protein binding
CD2AP	Actin binding
INF2	Cytoskeletal protein binding
SLC7A11	Transport protein

Abbreviation: DRGs, disulfidptosis-related genes.

by gene set variation analysis (GSVA) scores between different subtypes. Finally, the differences in immune cell infiltration between the different subtypes were compared.

Gene Co-Expression Network Construction

WGCNA was applied to select trait modules that are highly correlated with disease, which in turn identifies potential diagnostic biomarkers or targets for intervention.[15] First, hierarchical clustering was constructed on normal and UC samples to remove outlier samples according to the cutoff value of 0.8. Second, the adjacency matrix was built by the function pickSoft Threshold to select the optimal soft threshold of power. Afterward, the adjacency matrix was transformed into a topological overlap matrix (TOM), and then different gene modules were divided by dynamic tree cut. Subsequently, candidate modules associated with the characterized traits were identified by calculating module membership (MM) and gene significance (GS) for each module, and genes in candidate modules were screened based on MM > 0.8 and GS > 0.5. We used the same method for finding the gene modules of the subtype that were most associated with a specific trait. Finally, the hub genes from these two key modules were overlapped to obtain candidate signature genes by the "VennDiagram" R package.

Validation of Signature Genes

The expression levels of signature genes were evaluated with the test set (GSE75214 and GSE87473) and validation set (GSE36807) (P < 0.05). The diagnostic value of the signature genes in the dataset was assessed using the area under the curve (AUC) of the receiver operating characteristic (ROC) curve by the "pROC" R package.[16]

Construction of the Nomogram Model

Using the "rms" and "rmda" R packages, we constructed a nomogram model to predict the risk of UC from signature genes, and plotted calibration curves and DCA curves to assess the predictive accuracy of this model.

Single-Gene GSEA and ssGSEA

To further understand the molecular pathways with the signature genes in UC, GSEA was performed for the high and low expression groups based on the median expression of signature genes.[17] The top five positively regulated pathways were selected for presentation. Furthermore, the correlation between signature genes and 28 immune cells was assessed using Spearman's rank correlation coefficient (P < 0.05).

Single-Cell Analysis

To further explore the single-cell level of signature genes and DRGs in UC, we downloaded the GSE214695[18] dataset from the GEO database for single-cell sequencing analysis, which consists of six healthy control samples and six active UC samples. Expression profiles by high throughput sequencing were processed using the "Seurat" R package. Subsequently, PCA was used for dimensional reduction and cell clustering of highly variable genes. Then, the t-SNE algorithm was used to perform nonlinear dimensional reduction on the high-dimensional data. The "harmony" R package was used to reduce the batch effect among disease group and control group. The "SingleR" R package was used for cell annotation. The FindALLMarkers function filtered the marker genes for each cell subtype. Finally, we calculated the distribution and expression disparity of signature genes and DRGs in each cell cluster.

Sample Collection

We recruited 5 patients diagnosed with UC patients and 5 healthy control (HC) patients from the Gastroenterology Centre of Changzhou Second People's Hospital and performed intestinal mucosal biopsies from them during endoscopy. These recruited patients were informed about this study and signed an informed consent form before anesthesia. This study was approved by the Medical Ethics Committee of Changzhou Second People's Hospital and was conducted in accordance with the principles of the Declaration of Helsinki.

RNA Transcription and Real-Time PCR

We extracted total RNA from tissue samples of UC using an RNAiso plus kit (TaKaRa). Next, mRNA was reverse transcribed into complementary DNA (cDNA) by cDNA synthesis agent (Vazyme R222-01). This was followed by RT-qPCR using SYBR Green Master Mix reagent (Vazyme Q131). The relative data were determined using the $2^{-\Delta\Delta t}$ method, and β-actin was used as an internal control. The primer sequences for signature genes are presented in Table 2.

Result

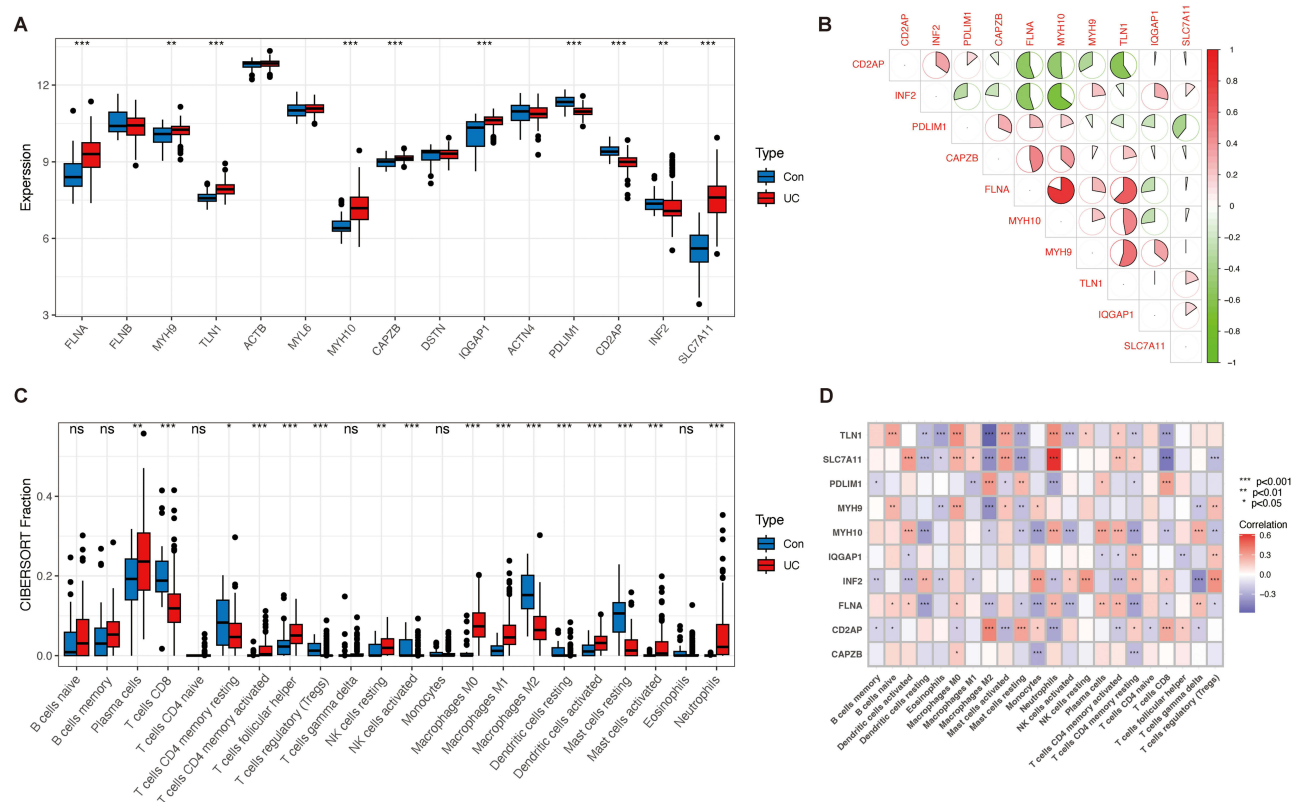## Screening of Disulfidptosis-Related Genes in UC

The GSE75214 and GSE87473 datasets were merged and their batch effects were eliminated, followed by the extraction of DRGs using the "limma" R package. Boxplots (Figure 3A) show the expression differences and distribution of the 15 DRGs in UC and control groups. In the gene expression profiles, *FLNA, MYH9, TLN1, MYH10, CAPZB, IQGAP1* and *SLC7A11* were significantly upregulated and *PDLIM1, CD2AP* and *INF2* were significantly downregulated. In addition, Figure 3B shows the correlation between the 10 DRGs.

Evaluation of Immune Cells Infiltration

To investigate the reasons for immune imbalance in UC and the function of DRGs in it, we calculated the proportions of different immune cells between UC and control groups using the CIBERSORT algorithm. Figure 3C suggests significant enrichment of plasma cells, T cells CD4 memory activate, NK cells resting, macrophages M0, macrophages M1 and neutrophils in UC. Correlation analysis of the 10 DRGs with immune cells revealed that *TLN1, MYH10, FLNA* and

Table 2 The Primer Sequences for PCR

Genes	Sequences (5'-3')	
COL4A1	Forward	TGTTGACGGCTTACCTGGAGAC
	Reverse	GGTAGACCAACTCCAGGCTCTC
PRRX1	Forward	CTGATGCTTTTGTGCGAGAA
	Reverse	ACTTGGCTCTTCGGTTCTGA
NNMT	Forward	ATTACAAGTTTGGTTCTAGGCACT
	Reverse	GGCCAGAGCCGATGTCAAT
PECAM1	Forward	GCATATCCAAGGTCAGCAGC
	Reverse	TCTGGATGGTGAAGTTGGCT

Figure 3 Identification of DRGs and Immune cell infiltration analysis in UC. (**A**) Boxplots showed the expression of 15 CRGs between UC and controls. (**B**) The correlation coefficients were marked with the area of the pie chart. (**C**) Boxplots shows the differences in immune cell infiltration between UC samples and control samples. (**D**) Correlation analysis between 10 differentially expressed DRGs and immune cells. *$P < 0.05$, **$P < 0.01$, ***$P < 0.001$, ns: no significant.
Abbreviations: UC, ulcerative colitis; Con, control.

SLC7A11 were positively correlated with T cells CD4 memory activated and neutrophils, and *PDLIM1, CD2AP* and *INF2* were negatively correlated with neutrophils (Figure 3D). These results imply that DRGs may influence the expression level of DRGs in UC through positively or negatively regulating relevant immune cells, which in turn affects development of UC.

Subtype Analysis with DRGs

According to the expression of seven upregulated DRGs, we clustered the 180 UC samples with consensus cluster analysis. Next, k = 2 was considered the optimal number of clusters based on the consensus matrix graph (Figure 4A), the CDF (cumulative distribution function) curve (Supplement Figure 1A), and the relative change in the area under the CDF curve (Supplement Figure 1B). Thus, we got two disulfidptosis related subtypes of UC, named cluster 1 (n = 81) and cluster 2 (n = 99). Then, PCA (Figure 4B) showed the clear differences between these two clusters. In addition, the boxplots and heatmaps (Figure 4C and D) suggest that the expression levels of *FLNA, MYH9, TLN1, MYH10*, and *CAPZB* were significantly higher in C2 than in C1. Immune infiltration analysis was performed for C1 and C2 by the CIBERSORT algorithm. Figure 4E shows that the levels of Plasma cells, T cells CD4 memory activated and Neutrophils infiltration remained significantly distinct between the two clusters. Finally, GSVA analysis (Figure 4F) mainly revealed that cluster 2 was enriched in galactose metabolism, lysine degradation, autoimmune thyroid disease, arginine and proline metabolism and asthma when compared to cluster1.

WGCNA of UC Samples and Subtypes

To find genes strongly associated with clinical traits, first, the top 25% of genes with the greatest fluctuations between UC samples and normal samples were selected for WGCNA analysis. After removing the abnormal samples, a power
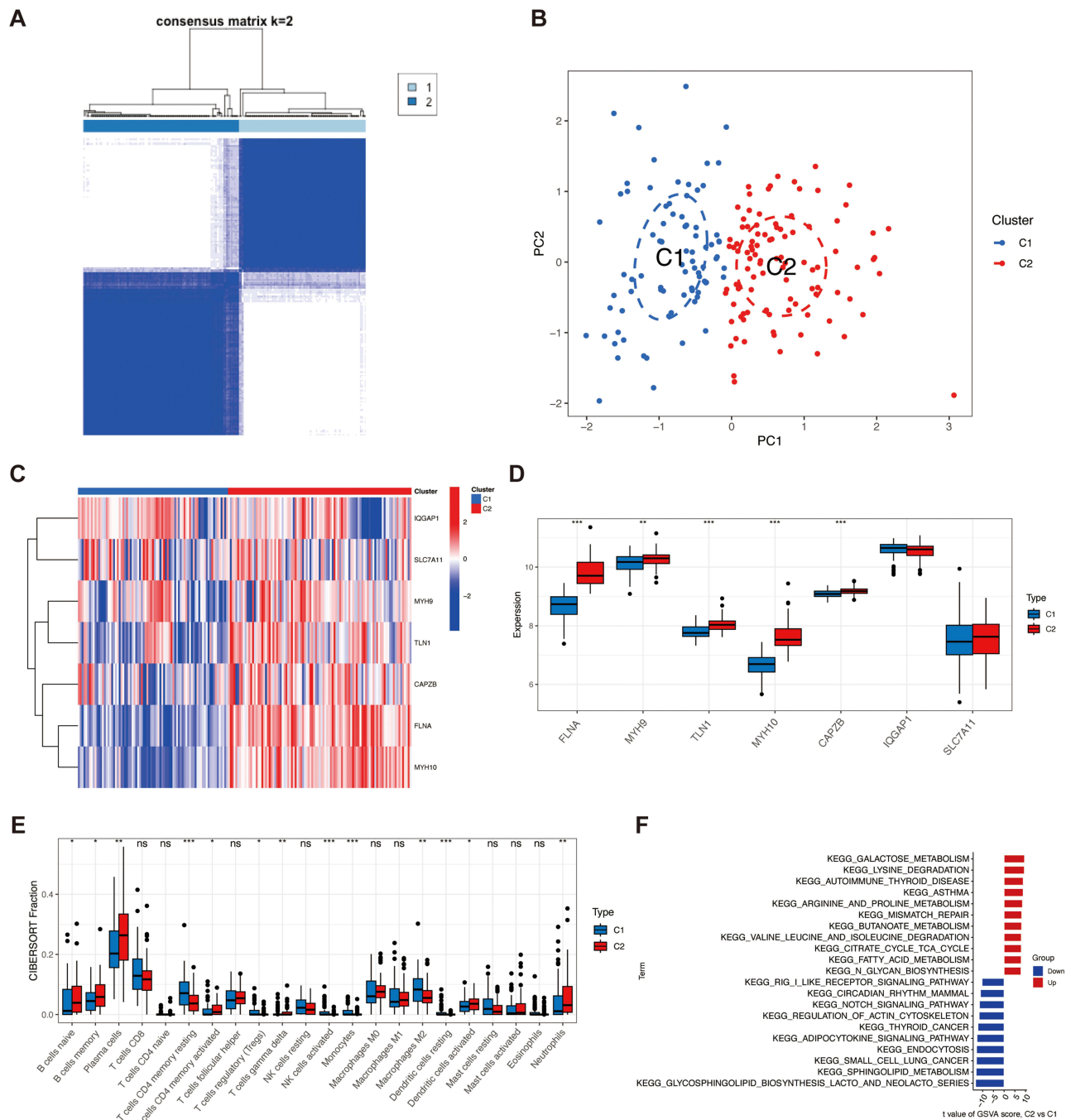
Figure 4 Identification of disulfidptosis-related subtypes in UC, and immune cell infiltration and GSVA analysis among two subtypes. (**A**) Consensus heatmaps when k = 2. (**B**) PCA of two subtypes. (**C**) Differential expression of 7 DRGs between subtypes is presented in the heatmap. (**D**) Boxplots shows the expression of 7 DRGs between two subtypes. (**E**) Boxplots shows the differences in immune cell infiltration between two subtypes. (**F**) GSVA analysis between cluster 1 and cluster 2. *$P < 0.05$, **$P < 0.01$, ***$P < 0.001$.
Abbreviations: C1, Cluster 1; C2, Cluster 2.

of β = 18 was chosen as the soft threshold based on the cutoff point equal to 0.8 to ensure the rationality of the scale-free network (Supplement Figure 2A). Subsequently, the dynamic cutting method identified seven modules of different colors. By analyzing the correlation between these module and clinical features (Figure 5A), the blue module (including 248 genes) was eventually identified as the most important gene module (Supplement Figure 2B). Similarly, we performed WGCNA on the two subtypes after clustering. A power of β = 18 was chosen as the soft
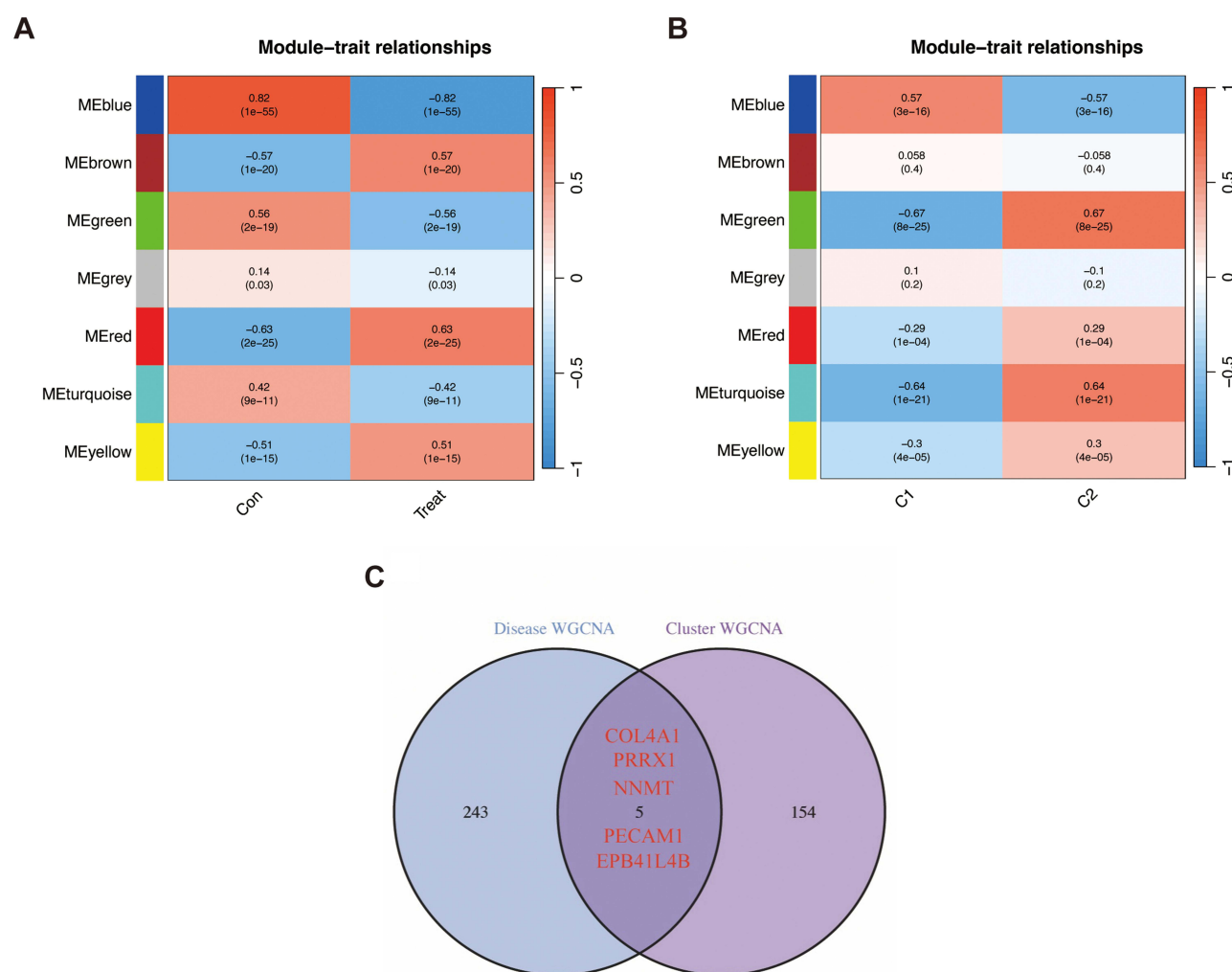
Figure 5 WGCNA selection of UC disease-related and cluster-related modules genes. (**A**) Heatmap of the correlation between module characteristic genes and UC. Blue and Red colors indicate negative and positive correlation, respectively. (**B**) Heatmap of the correlation between module characteristic genes and subtypes. (**C**) Overlap of genes between disease feature module and subtype feature module.
Abbreviations: Con, control; C1, Cluster 1; C2, Cluster 2.

threshold to identify modules with 7 different colors (Supplement Figure 2C). Based on the correlation between each module and the characteristics of the samples (Figure 5B), we found that the green module presented the highest correlation with cluster 2 and screened 159 genes in it (Supplement Figure 2D). After intersecting the genes in the blue module and green module, we identified 5 candidate signature genes (*COL4A1, EPB41L4B, PRRX1, NNMT*, and *PECAM1*) for subsequent analysis (Figure 5C).

Verification of Signature Genes and Construction of a Nomogram Model

In independent test sets, *COL4A1, PRRX1, NNMT* and *PECAM1* were found to be significantly upregulated in UC samples (Figure 6A–E) and the AUC values of four signature genes were all greater than 0.9 (Figure 6F–I). In validation set, the boxplots (Figure 7A–E) highlight the same results, and the AUC (Figure 7F–I) of signature genes also demonstrates high diagnostic efficacy. In this regard, we plotted a column line plots to predict the risk of UC based on signature genes (Figure 8A). In this model, the scores corresponding to each signature gene are summed to obtain a total score, which corresponds to the risk value of UC. Subsequently, the calibration curve (Figure 8B) and DCA curve (Figure 8C) suggested that the model presented a high prediction accuracy.
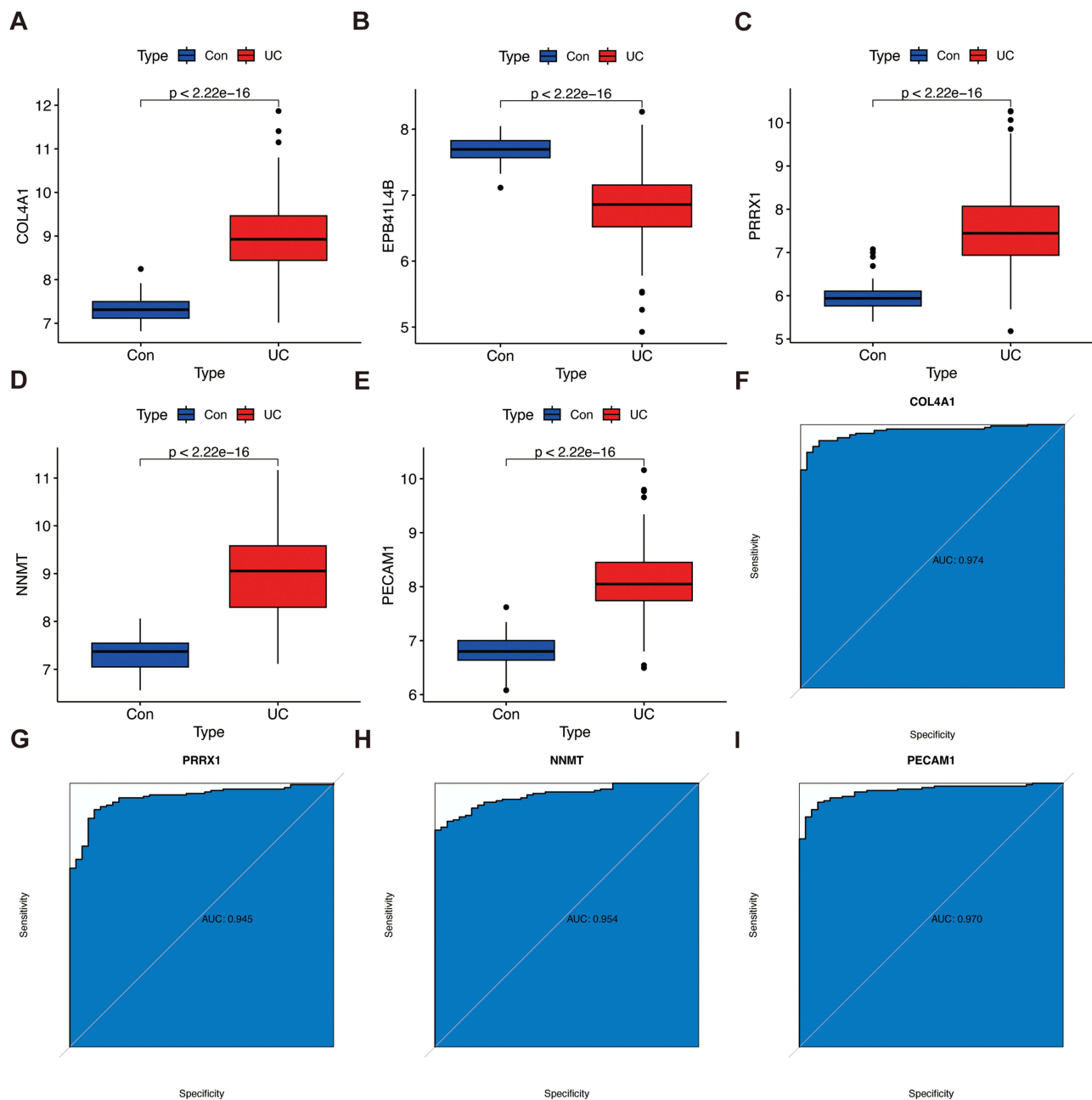
Figure 6 Expression level validation and diagnostic value in test set. (**A–E**) Expression level of COL4A1, EPB41L4B, PRRX1, NNMT, and PECAM1 in test set, respectively. (**F–I**) ROC curve of COL4A1, PRRX1, NNMT, and PECAM1 in test set, respectively.
Abbreviations: UC, ulcerative colitis; Con, control.

GSEA and ssGSEA

We performed GSEA analysis to explore the potential mechanisms of signature genes in UC, respectively. Notably, all signature genes were closely associated with allograft rejection, graft versus host disease and malaria (Figure 9A–D). From the results of the enrichment analysis, we found that signature genes may be related to the immune responses. Therefore, we continued to describe the correlation between the signature genes and association of these genes with 28 immune cells. Figure 9E demonstrates strong correlation between the hub genes. Figure 9F suggests that these genes are highly positively correlated with multiple immune cells. These results indicated that signature genes may be involved in the pathogenesis of UC by regulating a variety of immune cells and that there may be synergistic effects between the genes.
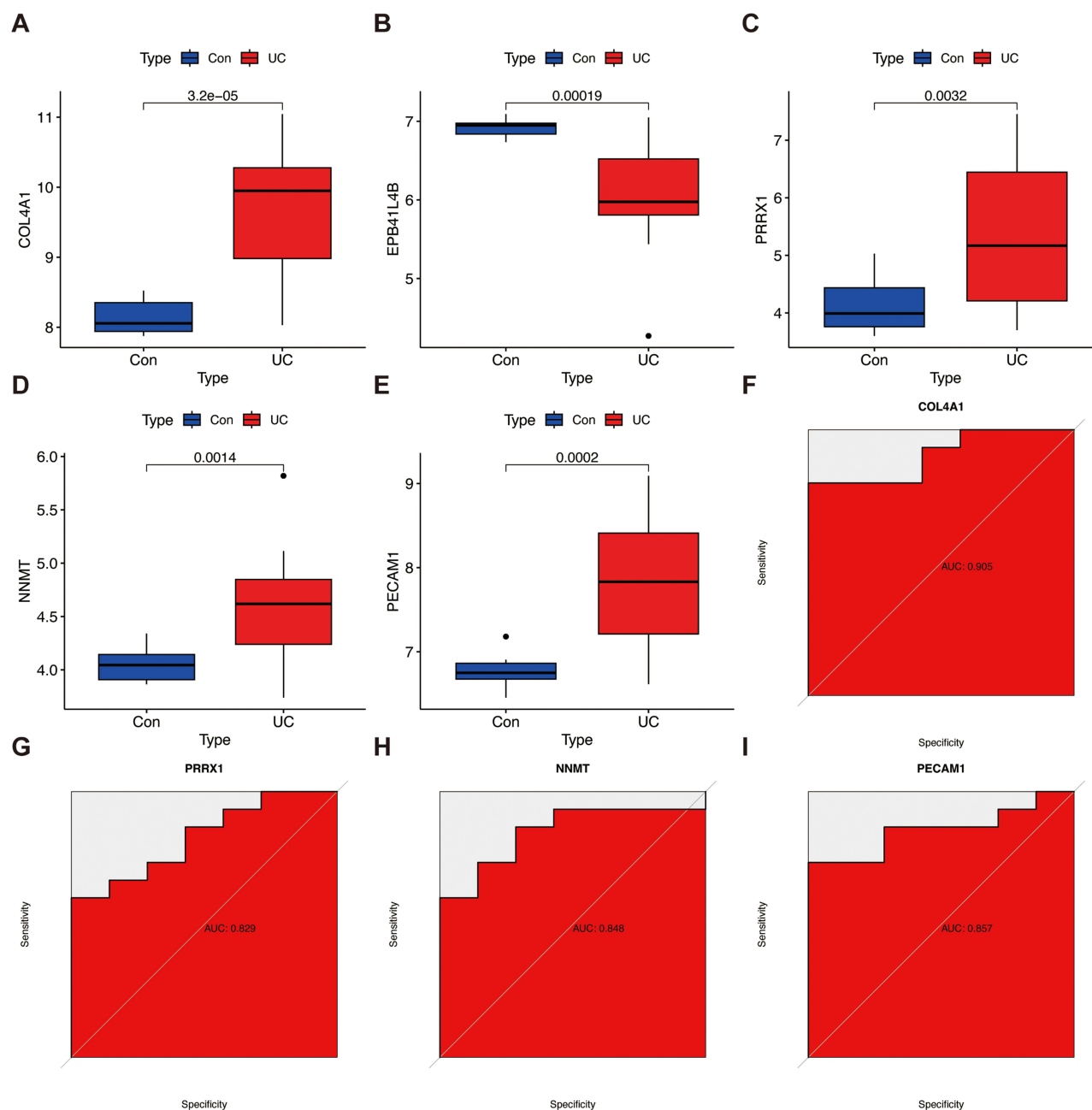
Figure 7 Expression level validation and diagnostic value in validation set. (**A–E**) Expression level of COL4A1, EPB41L4B, PRRX1, NNMT, and PECAM1 in validation set, respectively. (**F–I**) ROC curve of COL4A1, PRRX1, NNMT, and PECAM1 in validation set, respectively.
Abbreviations: UC, ulcerative colitis; Con, control.

Expression of Genes in Single Cells and Validation by qRT-PCR

We performed single-cell analysis of five UC tissue samples from the GSE214695 single-cell dataset using the "Seurat" R package. After clustering and dimensionality reduction of the screened cells by PCA and t-SNE algorithms, Figure 10A shows an overview of the single cell sequencing for the UC samples and the control samples. Figure 10B shows the expression level of the disulfidptosis gene set in UC samples and control samples. Afterwards, there were eight cell types were annotated, including B cells, T cells, monocyte, smooth muscle cells, epithelial cells, neutrophil, endothelial cells and NK cells (Figure 10C). Figure 10D shows the distribution of disulfidptosis-related genes in the 8 cell types. The violin plot for the expression disparity of disulfidptosis is shown in Figure 10E. The same algorithm was also used to investigate the expression of signature genes at the single-cell level. Figure 10F presents that signature genes
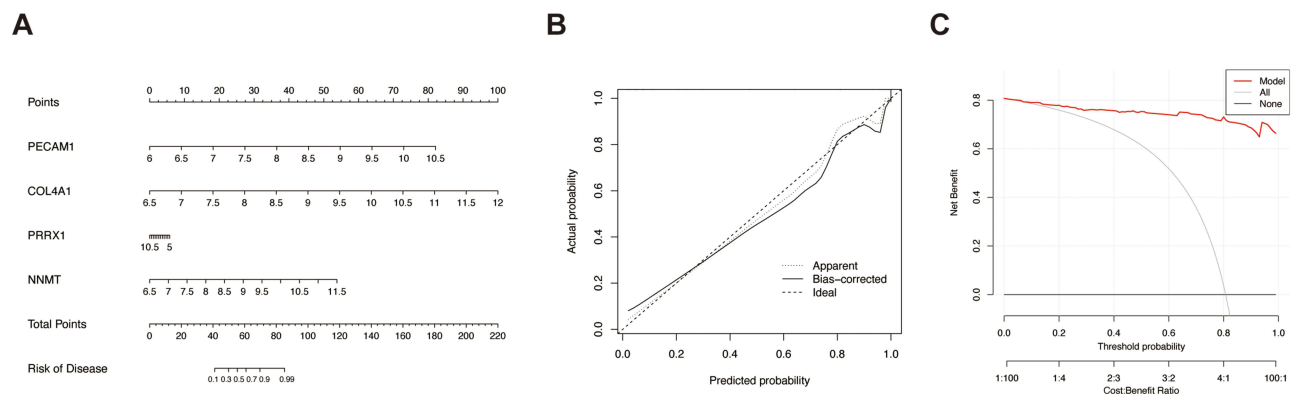
Figure 8 Predicting the risk of UC based on signature genes. (**A**) Creating a nomogram. Construction of calibration curve (**B**) and DCA (**C**) to evaluate the predictive efficiency of the nomogram model.

are mainly expressed in endothelial cells and smooth muscle cells. The violin plot for the expression disparity of signature genes is shown in Figure 10G. As shown in Figure 11A–D, consistent with the results of previous analysis, the signature genes are significantly expressed in UC samples. Therefore, these four genes can be considered as potential biomarkers for UC diagnosis.

Discussion

The incidence of UC has been increasing worldwide in recent years. Although mild and moderate UC patients account for the majority, the majority of patients have recurrent attacks, and the risk of cancer is significantly increased in some patients with a long course of disease, which undoubtedly places an enormous burden on the quality of life and economy of UC patients.[19] At present, the diagnosis of UC is mainly based on the patient's clinical features, endoscopy, and histopathology.[20] However, for some UC patients with atypical endoscopic changes and histopathological alterations, follow-up is needed for several months before making a diagnosis. Therefore, we need to explore new tools for the accurate diagnosis and prediction of UC development. This also provides new targets and therapeutic strategies for the future therapy of UC.

Disulfidptosis, as a unique cell death mode, provides important ideas for the treatment of multiple cancers. Studies have shown that during glucose starvation, abnormal accumulation of disulfide occurs in cells with high *SLC7A11* expression, which induces disulfide stress and rapid cell death.[7] In addition, GLUT inhibitors selectively induce cells with high *SLC7A11* expression to trigger disulfidptosis to inhibit tumor growth.[8] However, the role of disulfidptosis in UC is unknown. Therefore, for the first time, we attempted to analyze the potential association of disulfidptosis with UC from a bioinformatics perspective. In this study, we used unsupervised clustering and WGCNA to try to investigate the clinical application value of disulfidptosis in UC.

It is well known that intestinal immune imbalance is an important mechanism in the occurrence and development of UC that can lead to persistent inflammation of the intestinal mucosa and damage to barrier function.[6] Based on the results of immune cell infiltration, we found a significant difference in the proportion of immune cells between healthy and UC patients. Patients with UC had higher infiltration levels of CD4 T cells, NK cells, macrophages, and neutrophils compared to the normal group, which is also consistent with previous studies. Furthermore, a total of 10 DRGs were found to be abnormally different between the UC and control groups in this study. Subsequently, through evaluating the correlation of these 10 DRGs with immune cells, we identified four highly expressed DRGs (*TLN1, MYH10, FLNA*, and *SLC7A11*) that could promote the occurrence of UC by positively regulating CD4 T cells and neutrophils. As reported in the literature, these upregulated DRGs were mainly enriched in biological processes or pathways related to the actin cytoskeleton and cell adhesion.[7] Based on previous research, we found that these genes promote the growth, migration, and invasion of tumor cells. Notably, the actin cytoskeleton and cell adhesion are also strongly associated with colitis. In studies of colitis, integrin α4/β7 acts as a cell adhesion molecule, and its interaction with *MAdCAM-1* (mucosal address hormone cell adhesion molecule-1) caused T cells and B cells to enter the bowel, causing colitis to worsen.[21] In addition,
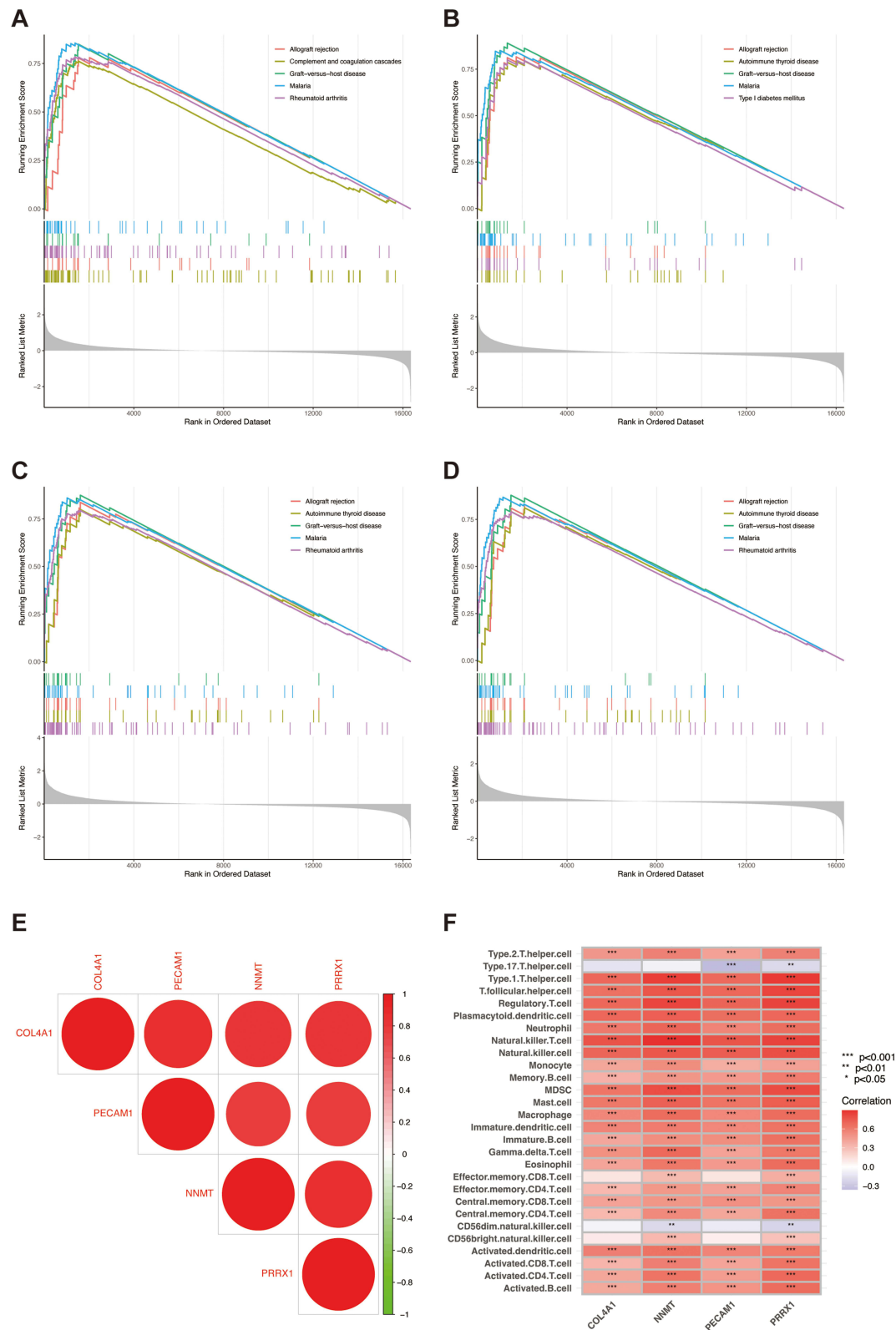
Figure 9 GSEA analysis of high expression and ssGSEA analysis in signature genes. (**A–D**) GSEA of COL4A1, PRRX1, NNMT, and PECAM1. (**E**) Correlation between signature genes. (**F**) Correlation between signature genes and 28 immune cells. *P < 0.05, **P < 0.01, ***P < 0.001.
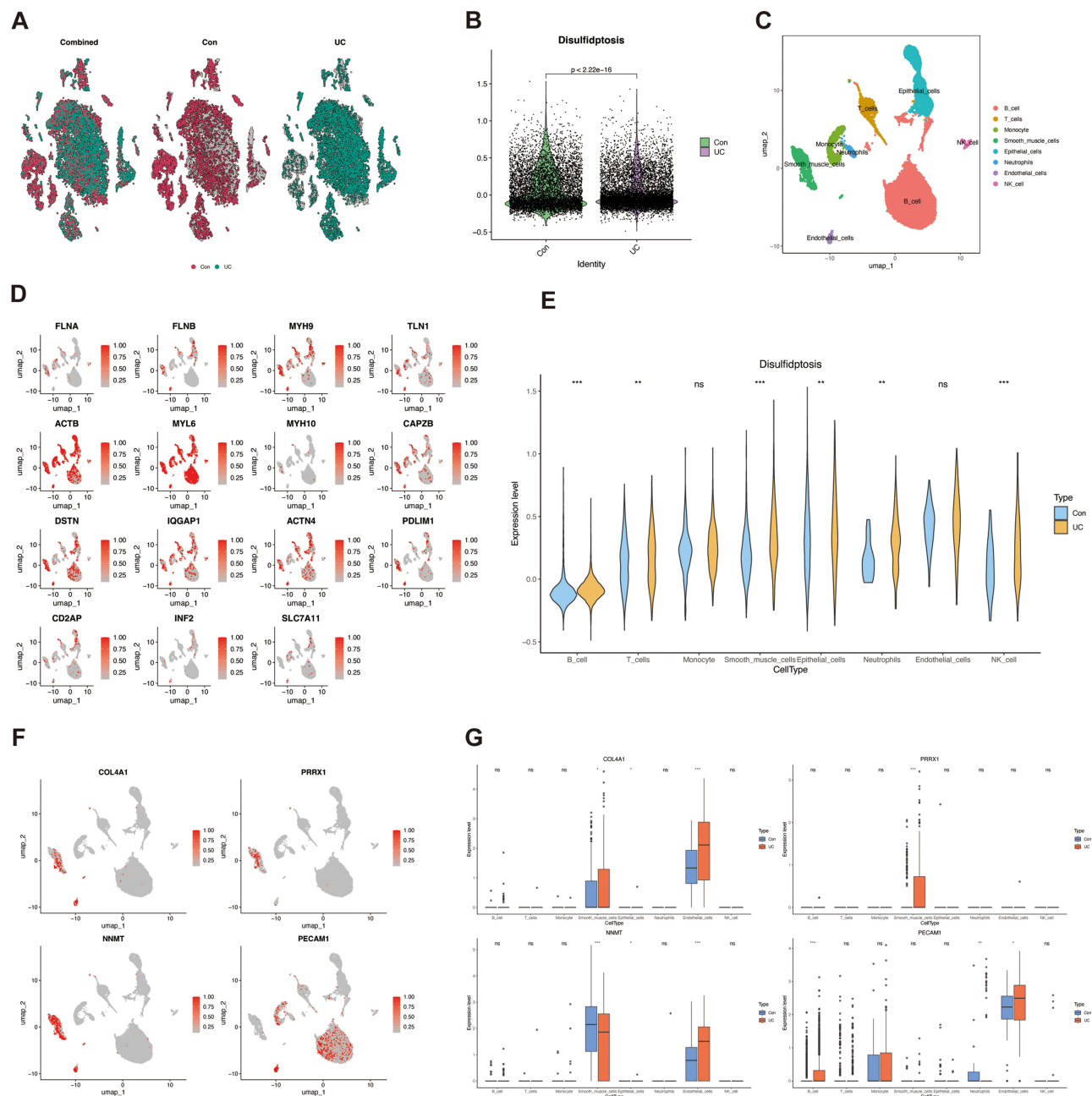
Figure 10 Overview of single cells from UC samples and control samples. (**A**) t-SNE of the UC samples and the control samples. (**B**) Expression level of disulfidptosis gene set in UC samples and control samples. (**C**) Cellular subtypes identified. (**D**) Feature plots showing disulfidptosis-related gene expressions in the 8 cell types. (**E**) Violin plot showing the expression disparity of disulfidptosis between UC and control groups. (**F**) Feature plots showing the signature gene expressions in the 8 cell types. (**G**) Violin plot showing the expression disparity of signature genes between UC and control groups. *$P < 0.05$, **$P < 0.01$, ***$P < 0.001$, ns: no significant.
Abbreviations: UC, ulcerative colitis; Con, control.

the actin cytoskeleton maintains the integrity of the intestinal mucosal barrier, when the expression level of *ROCK1* is abnormally upregulated, it leads to damage to the intestinal mucosal barrier by disrupting the formation of actin, thus promoting the occurrence of inflammatory bowel disease (IBD).[22] Therefore, we speculate that disulfidptosis-related genes may contribute to the worsening of colitis through similar pathological mechanisms. This preliminary evidence will be essential in understanding the association of disulfidptosis with UC.

In order to get insight into the heterogeneity of UC at the molecular level, we used an unsupervised clustering method based on 7 upregulated DRGs to categorize UC samples into two subtypes, the low-disufidptosis group (C1) and the
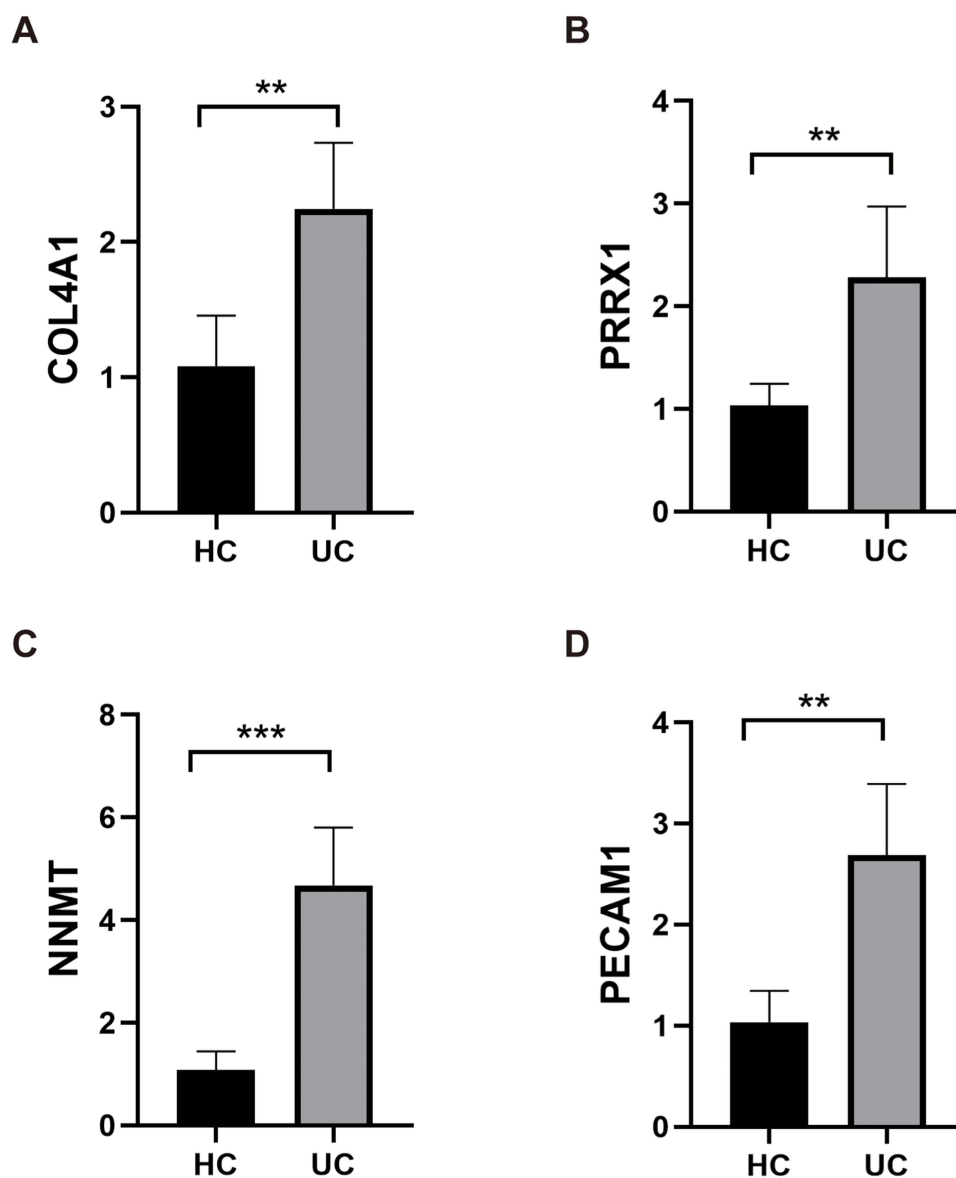
A

B

C

D

Figure 11 The result of Real-time PCR analysis illustrated the expression levels of signature genes (**A-D**) in patients with UC (n = 5) and HC (n = 5). *******P* < 0.01, ********P* < 0.001.
Abbreviations: UC, ulcerative colitis; HC, Healthy control.

high-disulphidptosis group (C2). According to the results of the immune infiltration analysis, this study found that the immune cellular and molecular pathways that influence the development of UC differ between subgroups. For example, the levels of infiltration of NK cells, monocytes, and macrophages M2 were higher in C1; B cells, plasma cells, and neutrophils were higher in C2. In addition, in GSVA analysis, C2 was mainly enriched in galactose metabolism, lysine degradation and autoimmune thyroid disease pathways; C1 was mainly enriched in glycosphingolipid biosynthesis lacto and neolacto series, sphingolipid metabolism and small cell lung cancer pathways. Therefore, in subsequent studies, we can help researchers to target different subgroups for precise treatment in terms of pathophysiology through the results of immune cell infiltration and pathway enrichment. After clustering the samples, there were still five upregulated DRGs that demonstrated higher expression levels in C2. Subsequently, we performed WGCNA on UC samples and subtypes, intersecting two key modules to obtain signature genes. After validation, *COL4A1, PRRX1, NNMT*, and *PECAM1* were identified as the most important signature genes for diagnosing UC. The nomogram model constructed from these four genes had a high potential to predict the risk of UC. Based on single-gene GSEA, we found that these genes mainly

influence disease development through immune-related pathways and correlation analysis suggested a high positive correlation between the four hub genes. Moreover, the results of ssGSEA analysis further demonstrated that hub genes are positively associated with multiple immune cells. Therefore, the present study suggested that the signature genes may contribute to the progression of UC by positively regulating immune cells that a mutually promoting effect may exist between these genes.

COL4A1 (type IV collagen α1) is the most abundant component of basement membrane,[23] and *COL4A1* mutations lead to the emergence of diverse disorders in clinical practice, including myopathy, glaucoma, and hemorrhagic stroke.[24] Moreover, *COL4A1* was dramatically upregulated in the development of cardiac fibrosis,[25] renal fibrosis,[26] and pulmonary fibrosis.[27] In a study of transcriptome analysis, the extracellular matrix (ECM) related gene *COL4A1* was significantly expressed in patients with Crohn's disease (CD). We consider that this may be associated with CD promoting intestinal fibrosis.[28] The transcription factor *PRRX1* (paired related homeobox 1) regulates gene expression in various physiological and pathological processes, including embryonic and skeletal development, cancer progression, and inflammation.[29–31] In studies of colitis, *PRRX1* activated *MMP13* and then promoted DSS-induced (dextran sulfate sodium) cellular inflammation and gut barrier dysfunction.[32] Nicotinamide N-methyltransferase (*NNMT*) is a newly discovered viable therapeutic target for the treatment of cancers.[33] According to a previous report, *NNMT* could be overexpressed in a variety of cancer diseases, promoting the migration, invasion, and proliferation of cancer cells.[34] Furthermore, high expression of *NNMT* also contributes to metabolic diseases,[35] neurodegenerative disorders,[36] and functional disorders of the endothelium.[37] The study demonstrated that *NNMT* could maintain high levels of NAD-dependent (nicotinamide adenine dinucleotide) proinflammatory signaling through the removal of excess inhibitory Nam (nicotinamide) thereby exacerbating the progression of colitis in mice.[38] Therefore, *NNMT* was considered by them as an alternative drug therapeutic target for IBD, which is also similar to the findings of this study. Platelet endothelial cell adhesion molecule-1 (*PECAM1/CD31*) was a member of the immunoglobulin superfamily (IgSF). *PECAM1* was involved with the proinflammatory process by promoting leukocyte migration to the site of inflammation to cause tissue damage[39] and the expression of *PECAM1* was upregulated in monocytes, neutrophils, T-cell subsets, and B cells.[40,41] In the study of infliximab for IBD, *PECAM1* was identified as a novel target for anti-adhesion therapy.[42] In summary, the four signature genes identified in this study are strongly associated with the pathogenesis of UC, and all of them can be used as target genes for early diagnosis and early treatment of UC.

In closing, we performed single-cell sequencing analysis of 6 UC and 6 control tissues to illustrate the underlying mechanisms of heterogeneity in UC and further explore the expression of DRGs and signature genes in disease. In this work, a total of eight cell types (B cells, T cells, monocyte, smooth muscle cells, epithelial cells, neutrophil, endothelial cells and NK cells) were annotated after clustering. We found that DRGs were predominantly expressed at higher levels in UC samples and that the majority of DRGs were expressed in endothelial cells. These findings will improve the understanding of disulfidptosis in UC and provide a foundation for subsequent fundamental research. The signature genes (*COL4A1, PRRX1, NNMT* and *PECAM1*), they were differentially expressed mainly in smooth muscle cells (SMCs) and endothelial cells (ECs). It was found that inflammation induces SMCs proliferation leading to changes in their phenotype.[43] Understanding the mechanisms underlying the phenotypic shift of intestinal SMCs could help to minimize the adverse effects of intestinal inflammation. A study demonstrated that *NR4A1* inhibits inflammation related intestinal fibrous strictures by mediating the intestinal SMCs phenotype.[44] In addition, the function of ECs (regulation of immune cells and angiogenesis) was considered a key element in the pathological mechanism of IBD, which mediates and exacerbates inflammation in intestine.[45,46] Thus, several studies have proposed new strategies to treat IBD by targeting multiple integrins and adhesion molecules expressed on ECs.[47,48] The above evidence indicated that not only immune cells play a crucial role in UC, but also SMCs and ECs are key factors in regulating intestinal inflammation, which provides reliable evidence for the pathogenesis of UC in the future.

In addition, this study also has several limitations. First, the results of this study were dependent on bioinformatics analysis and qRT-PCR validation. Therefore, we need more cell biology experiments and animal experiments are needed for verification in future. Second, our study collected relatively few UC samples, so we need to conduct multi-sample studies to verify the reliability of the results. Finally, the studies on the above seven upregulated DRGs in UC are relatively few, and further functional experiments are needed to validate their mechanisms and clinical value in UC.

Conclusion

In conclusion, this study identified seven disulfidptosis-related genes with upregulated expression in patients with UC and revealed their correlation with immune cells. In addition, we identified 4 signature genes (*COL4A1, PRRX1, NNMT* and *PECAM1*) based on subtypes and WGCNA and constructed a nomogram model that accurately predicted the risk of UC. In single-cell RNA sequencing, we found that signature genes were differentially expressed mainly in endothelial cells and smooth muscle cells. Our study reveals for the first time the value of disulfidptosis in UC to effectively address the underlying mechanisms and therapeutic strategies of UC.

Acknowledgments

Author Contributions

All authors made a significant contribution to the work reported, whether that is in the conception, study design, execution, acquisition of data, analysis and interpretation, or in all these areas; took part in drafting, revising or critically reviewing the article; gave final approval of the version to be published; have agreed on the journal to which the article has been submitted; and agree to be accountable for all aspects of the work.

Disclosure

All authors report no conflicts of interest in this work.

References

1. Ordás I, Eckmann L, Talamini M, Baumgart DC, Sandborn WJ. Ulcerative colitis. *Lancet*. 2012;380(9853):1606–1619. doi:10.1016/s0140-6736(12)60150-0

2. Ng SC, Shi HY, Hamidi N, et al. Worldwide incidence and prevalence of inflammatory bowel disease in the 21st century: a systematic review of population-based studies. *Lancet*. 2017;390(10114):2769–2778. doi:10.1016/s0140-6736(17)32448-0

3. Sun Y, Zhang Z, Zheng CQ, Sang LX. Mucosal lesions of the upper gastrointestinal tract in patients with ulcerative colitis: a review. *World J Gastroenterol*. 2021;27(22):2963–2978. doi:10.3748/wjg.v27.i22.2963

4. Shah SC, Itzkowitz SH. Colorectal Cancer in Inflammatory Bowel Disease: mechanisms and Management. *Gastroenterology*. 2022;162(3):715–730.e3. doi:10.1053/j.gastro.2021.10.035

5. de Souza HS, Fiocchi C. Immunopathogenesis of IBD: current state of the art. *Nat Rev Gastroenterol Hepatol*. 2016;13(1):13–27. doi:10.1038/nrgastro.2015.186

6. Oshi MA, Naeem M, Bae J, et al. Colon-targeted dexamethasone microcrystals with pH-sensitive chitosan/alginate/Eudragit S multilayers for the treatment of inflammatory bowel disease. *Carbohydr Polym*. 2018;198:434–442. doi:10.1016/j.carbpol.2018.06.107

7. Liu X, Nie L, Zhang Y, et al. Actin cytoskeleton vulnerability to disulfide stress mediates disulfidptosis. *Nat Cell Biol*. 2023;25(3):404–414. doi:10.1038/s41556-023-01091-2

8. Zheng P, Zhou C, Ding Y, Duan S. Disulfidptosis: a new target for metabolic cancer therapy. *J Exp Clin Cancer Res*. 2023;42(1):103. doi:10.1186/s13046-023-02675-4

9. Vancamelbeke M, Vanuytsel T, Farré R, et al. Genetic and transcriptomic bases of intestinal epithelial barrier dysfunction in inflammatory bowel disease. *Inflamm Bowel Dis*. 2017;23(10):1718–1729. doi:10.1097/mib.0000000000001246

10. Li K, Strauss R, Ouahed J, et al. Molecular comparison of adult and pediatric ulcerative colitis indicates broad similarity of molecular pathways in disease tissue. *J Pediatr Gastroenterol Nutr*. 2018;67(1):45–52. doi:10.1097/mpg.0000000000001898

11. Montero-Meléndez T, Llor X, García-Planella E, Perretti M, Suárez A. Identification of novel predictor classifiers for inflammatory bowel disease by gene expression profiling. *PLoS One*. 2013;8(10):e76235. doi:10.1371/journal.pone.0076235

12. Newman AM, Liu CL, Green MR, et al. Robust enumeration of cell subsets from tissue expression profiles. *Nat Methods*. 2015;12(5):453–457. doi:10.1038/nmeth.3337

13. Wilkerson MD, Hayes DN. ConsensusClusterPlus: a class discovery tool with confidence assessments and item tracking. *Bioinformatics*. 2010;26(12):1572–1573. doi:10.1093/bioinformatics/btq170

14. Ritchie ME, Phipson B, Wu D, et al. limma powers differential expression analyses for RNA-sequencing and microarray studies. *Nucleic Acids Res*. 2015;43(7):e47. doi:10.1093/nar/gkv007

15. Langfelder P, Horvath S. WGCNA: an R package for weighted correlation network analysis. *BMC Bioinf*. 2008;9:559. doi:10.1186/1471-2105-9-559

16. Robin X, Turck N, Hainard A, et al. pROC: an open-source package for R and S+ to analyze and compare ROC curves. *BMC Bioinf*. 2011;12:77. doi:10.1186/1471-2105-12-77

17. Hänzelmann S, Castelo R, Guinney J. GSVA: gene set variation analysis for microarray and RNA-seq data. *BMC Bioinf*. 2013;14:7. doi:10.1186/1471-2105-14-7

18. Garrido-Trigo A, Corraliza AM, Veny M, et al. Macrophage and neutrophil heterogeneity at single-cell spatial resolution in human inflammatory bowel disease. *Nat Commun*. 2023;14(1):4506. doi:10.1038/s41467-023-40156-6

19. Olén O, Erichsen R, Sachs MC, et al. Colorectal cancer in ulcerative colitis: a Scandinavian population-based cohort study. *Lancet*. 2020;395 (10218):123–131. doi:10.1016/s0140-6736(19)32545-0

20. Conrad K, Roggenbuck D, Laass MW. Diagnosis and classification of ulcerative colitis. *Autoimmun Rev*. 2014;13(4–5):463–466. doi:10.1016/j. autrev.2014.01.028

21. Tyler CJ, Guzman M, Lundborg LR, et al. Antibody secreting cells are critically dependent on integrin α4β7/MAdCAM-1 for intestinal recruitment and control of the microbiota during chronic colitis. *Mucosal Immunol*. 2022;15(1):109–119. doi:10.1038/s41385-021-00445-z

22. Kang S, Kim J, Park A, et al. TRIM40 is a pathogenic driver of inflammatory bowel disease subverting intestinal barrier integrity. *Nat Commun*. 2023;14(1):700. doi:10.1038/s41467-023-36424-0

23. Kalluri R. Basement membranes: structure, assembly and role in tumour angiogenesis. *Nat Rev Cancer*. 2003;3(6):422–433. doi:10.1038/nrc1094

24. Kuo DS, Labelle-Dumais C, Gould DB. COL4A1 and COL4A2 mutations and disease: insights into pathogenic mechanisms and potential therapeutic targets. *Hum Mol Genet*. 2012;21(R1):R97–110. doi:10.1093/hmg/dds346

25. Chen S, Puthanveetil P, Feng B, Matkovich SJ, Dorn GW, Chakrabarti S. Chakrabarti S. Cardiac miR-133a overexpression prevents early cardiac fibrosis in diabetes. *J Cell Mol Med*. 2014;18(3):415–421. doi:10.1111/jcmm.12218

26. Solé C, Moliné T, Vidal M, Ordi-Ros J, Cortés-Hernández J. An Exosomal Urinary miRNA Signature for Early Diagnosis of Renal Fibrosis in Lupus Nephritis. *Cells*. 2019;8(8):773. doi:10.3390/cells8080773

27. Savin IA, Markov AV, Zenkova MA, Sen'kova AV. Asthma and post-asthmatic fibrosis: a search for new promising molecular markers of transition from acute inflammation to pulmonary fibrosis. *Biomedicines*. 2022;10(5):1017. doi:10.3390/biomedicines10051017

28. Eshelman MA, Harris L, Deiling S, Koltun WA, Jeganathan NA, Yochum GS. Transcriptomic analysis of ileal tissue from Crohn's disease patients identifies extracellular matrix genes that distinguish individuals by age at diagnosis. *Physiol Genomics*. 2020;52(10):478–484. doi:10.1152/physiolgenomics.00062.2020

29. Yang R, Liu Y, Wang Y, et al. Low PRRX1 expression and high ZEB1 expression are significantly correlated with epithelial-mesenchymal transition and tumor angiogenesis in non-small cell lung cancer. *Medicine*. 2021;100(4):e24472. doi:10.1097/md.0000000000024472

30. Kern MJ, Argao EA, Birkenmeier EH, Rowe LB, Potter SS. Genomic organization and chromosome localization of the murine homeobox gene Pmx. *Genomics*. 1994;19(2):334–340. doi:10.1006/geno.1994.1066

31. Dankel SN, Grytten E, Bjune JI, et al. COL6A3 expression in adipose tissue cells is associated with levels of the homeobox transcription factor PRRX1. *Sci Rep*. 2020;10(1):20164. doi:10.1038/s41598-020-77406-2

32. Zhang X, Ma L, Shen Y, Zhang C, Hou B, Zhou Y. Transcription factor paired related homeobox 1 (PRRX1) activates matrix metalloproteinases (MMP)13, which promotes the dextran sulfate sodium-induced inflammation and barrier dysfunction of NCM460 cells. *Bioengineered*. 2022;13 (1):645–654. doi:10.1080/21655979.2021.2012549

33. Gao Y, Martin NI, van Haren MJ. Nicotinamide N-methyl transferase (NNMT): an emerging therapeutic target. *Drug Discov Today*. 2021;26 (11):2699–2706. doi:10.1016/j.drudis.2021.05.011

34. Ulanovskaya OA, Zuhl AM, Cravatt BF. NNMT promotes epigenetic remodeling in cancer by creating a metabolic methylation sink. *Nat Chem Biol*. 2013;9(5):300–306. doi:10.1038/nchembio.1204

35. Liu M, Li L, Chu J, et al. Serum N(1)-methylnicotinamide is associated with obesity and diabetes in Chinese. *J Clin Endocrinol Metab*. 2015;100 (8):3112–3117. doi:10.1210/jc.2015-1732

36. Schmeisser K, Parker JA. Nicotinamide-N-methyltransferase controls behavior, neurodegeneration and lifespan by regulating neuronal autophagy. *PLoS Genet*. 2018;14(9):e1007561. doi:10.1371/journal.pgen.1007561

37. Fedorowicz A, Mateuszuk Ł, Kopec G, et al. Activation of the nicotinamide N-methyltransferase (NNMT)-1-methylnicotinamide (MNA) pathway in pulmonary hypertension. *Respir Res*. 2016;17(1):108. doi:10.1186/s12931-016-0423-7

38. Wnorowski A, Wnorowska S, Kurzepa J, Parada-Turska J. Alterations in Kynurenine and NAD(+) salvage pathways during the successful treatment of inflammatory bowel disease suggest HCAR3 and NNMT as potential drug targets. *Int J Mol Sci*. 2021;22:24.

39. Woodfin A, Voisin MB, Nourshargh S. PECAM-1: a multi-functional molecule in inflammation and vascular biology. *Arterioscler Thromb Vasc Biol*. 2007;27(12):2514–2523. doi:10.1161/atvbaha.107.151456

40. Govender D, Harilal P, Dada M, Chetty R. CD31 (JC70) expression in plasma cells: an immunohistochemical analysis of reactive and neoplastic plasma cells. *J Clin Pathol*. 1997;50(6):490–493. doi:10.1136/jcp.50.6.490

41. Baumann CI, Bailey AS, Li W, Ferkowicz MJ, Yoder MC, Fleming WH. PECAM-1 is expressed on hematopoietic stem cells throughout ontogeny and identifies a population of erythroid progenitors. *Blood*. 2004;104(4):1010–1016. doi:10.1182/blood-2004-03-0989

42. Arijs I, De Hertogh G, Machiels K, et al. Mucosal gene expression of cell adhesion molecules, chemokines, and chemokine receptors in patients with inflammatory bowel disease before and after infliximab treatment. *Am J Gastroenterol*. 2011;106(4):748–761. doi:10.1038/ajg.2011.27

43. Bonafiglia QA, Lourenssen SR, Hurlbut DJ, Blennerhassett MG. Epigenetic modification of intestinal smooth muscle cell phenotype during proliferation. *Am J Physiol Cell Physiol*. 2018;315(5):C722–c733. doi:10.1152/ajpcell.00216.2018

44. Szczepanski HE, Flannigan KL, Mainoli B, et al. NR4A1 modulates intestinal smooth muscle cell phenotype and dampens inflammation-associated intestinal remodeling. *FASEB j*. 2022;36(11):e22609. doi:10.1096/fj.202101817RR

45. Cromer WE, Mathis JM, Granger DN, Chaitanya GV, Alexander JS. Role of the endothelium in inflammatory bowel diseases. *World J Gastroenterol*. 2011;17(5):578–593. doi:10.3748/wjg.v17.i5.578

46. Danese S, Dejana E, Fiocchi C. Immune regulation by microvascular endothelial cells: directing innate and adaptive immunity, coagulation, and inflammation. *J Immunol*. 2007;178(10):6017–6022. doi:10.4049/jimmunol.178.10.6017

47. Danese S, Panés J. Development of drugs to target interactions between leukocytes and endothelial cells and treatment algorithms for inflammatory bowel diseases. *Gastroenterology*. 2014;147(5):981–989. doi:10.1053/j.gastro.2014.08.044

48. Slack RJ, Macdonald SJF, Roper JA, Jenkins RG, Hatley RJD. Emerging therapeutic opportunities for integrin inhibitors. *Nat Rev Drug Discov*. 2022;21(1):60–78. doi:10.1038/s41573-021-00284-4